ACS MATERIALS Au
AN OPEN ACCESS JOURNAL OF THE AMERICAN CHEMICAL SOCIETY

pubs.acs.org/materialsau

Perspective

Magic-Size Semiconductor Nanostructures: Where Does the Magic Come from?

Serena Busatto and Celso de Mello Donega*

Cite This: *ACS Mater. Au* 2022, 2, 237−249

Read Online

ACCESS | Metrics & More | Article Recommendations

ABSTRACT: The quest for atomically precise synthesis of colloidal semiconductor nanostructures has attracted increasing attention in recent years and remains a formidable challenge. Nevertheless, atomically precise clusters of semiconductors, known as magic-size clusters (MSCs), are readily accessible. Ultrathin one-dimensional nanowires and two-dimensional nanoplatelets and nanosheets can also be categorized as magic-size nanocrystals (MSNCs). Further, the magic-size growth regime has been recently extended into the size range of colloidal QDs (up to 3.5 nm). Nevertheless, the underlying reasons for the enhanced stability of magic-size nanostructures and their formation mechanisms remain obscure. In this Perspective, we address these intriguing questions by critically analyzing the currently available knowledge on the formation and stability of both MSCs and MSNCs (0D, 1D, and 2D). We conclude that research on magic-size colloidal nanostructures is still in its infancy, and many fundamental questions remain unanswered. Nonetheless, we identify several correlations between the formation of MSCs and 0D, 1D and 2D MSNSs. From our analysis, it appears that the "magic" originates from the complexity of a dynamic and multivariate system running under reaction control. Under conditions that impose a prohibitively high energy barrier for classical nucleation and growth, the reaction proceeds through a complex and dynamic potential landscape, searching for the pathway with the lowest energy barrier, thereby sequentially forming metastable products as it jumps from one local minimum to the next until it eventually becomes trapped into a minimum that is too deep with respect to the available thermal energy. The intricacies of this complex interplay between several synergistic and antagonistic processes are, however, not yet understood and should be further investigated by carefully designed experiments combining multiple complementary in situ characterization techniques.

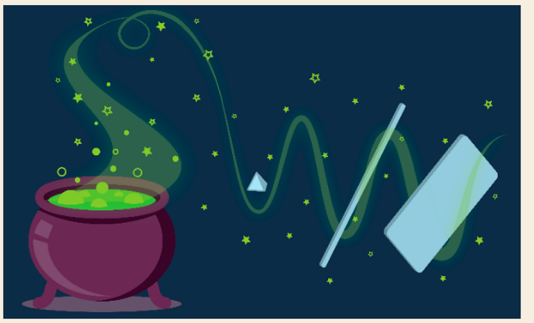

KEYWORDS: *Magic-Size Clusters, Ultrathin Nanowires, Nanosheets, Nanoplatelets, II−VI semiconductors, III−V Semiconductors, CdSe, InP*

1. INTRODUCTION

Colloidal semiconductor nanocrystals (NCs) are versatile nanomaterials, whose optoelectronic properties are determined by their size, shape, composition, and compositional profile.[1,2] The size and shape dependence of their properties emerges from the spatial confinement of charge carriers and excitons in the material, resulting in quantum confinement effects. The impact of these effects is determined by a material-dependent characteristic length scale given by the exciton Bohr radius (a_0), which ranges from ∼2 to ∼50 nm depending on the semiconductor (Figure 1).[3,4] The degree of quantum confinement may vary in different directions depending on the NC shape and size, yielding zero-dimensional (0D) quantum dots (QDs), one-dimensional (1D) nanowires, and two-dimensional (2D) nanosheets (Figure 1).[3] Quasi-1D (i.e., weak confinement occurs also in the length direction, e.g., nanorods) and quasi-2D (i.e., weak confinement occurs also in the lateral directions, e.g., nanoribbons and nanoplatelets) can also be prepared.[4]

Another important characteristic of colloidal semiconductor NCs is that they are coated with a layer of organic ligand molecules (Figure 1).[1] The ligands have a crucial impact on the properties of colloidal NCs, defining their size and shape during the synthesis and their postsynthetic colloidal stability. As a result, one can take full advantage of nanoscale effects to combine property tailoring through size, shape, and composition control with easy surface functionalization and solution processing.[1] This prospect has turned colloidal semiconductor NCs into attractive materials for several existing and emergent applications.[5−11] However, the realization of this bright potential has been hindered by both the intrinsic toxicity

Received: November 28, 2021
Revised: January 12, 2022
Accepted: January 13, 2022
Published: January 28, 2022

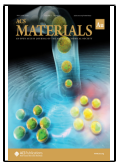

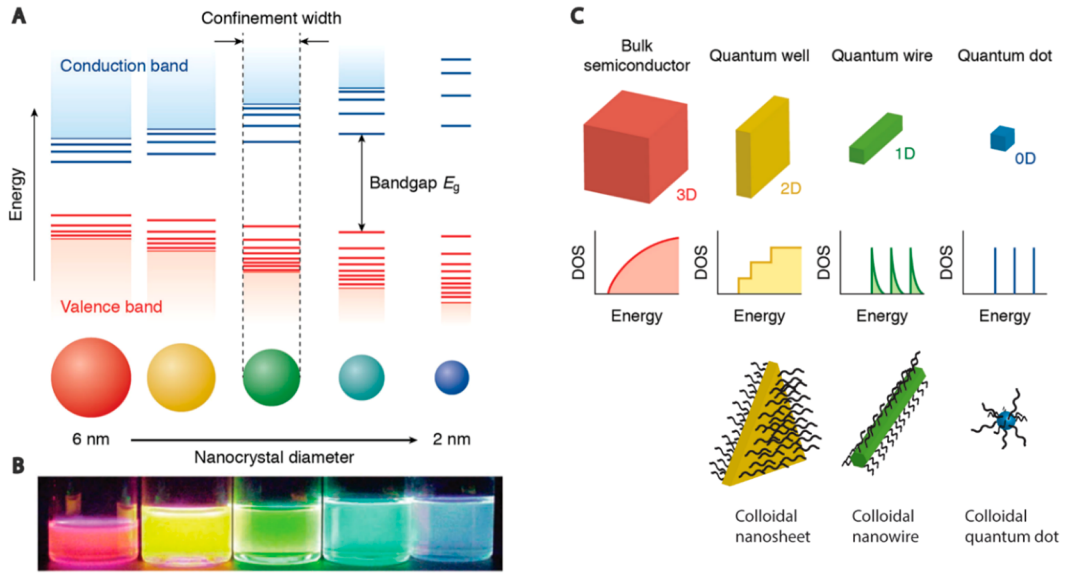

Figure 1. (A) Schematic representation of quantum confinement effects. (B) Colloidal dispersions of CdSe NCs with different sizes under UV illumination. The NC size decreases from left to right (6 to 2 nm), and the corresponding increase in the band gap is reflected in the change of the photoluminescence color. (C) Schematic representation of the energy level structure of a bulk semiconductor and of semiconductor nanostructures with reduced dimensionality from 2D (exciton is confined only in the thickness dimension) to 1D (exciton is confined in the diameter direction) to 0D (exciton is confined in all directions) (DOS: density of electronic states). Colloidal NCs capped with organic ligands can be made with dimensionality ranging from 2D to 0D (bottom panel). Reproduced from ref 4. Copyright 2017 American Chemical Society.

of the best developed colloidal NCs, which are based on Cd- and Pb-chalcogenides, and the relatively large polydispersity of ensembles of NCs of alternative semiconductors. This has driven both the development of alternative colloidal NCs based on nontoxic (or less toxic) elements (for example, InP,[2,12] InSb,[13] or $CuAX_2$,[2,14] with A = In, Ga and X = S, Se) and a quest for atomically precise synthesis, yielding monodisperse ensembles of NCs.[15−17] In this Perspective, we address topics that are relevant to the latter, which remains a formidable challenge.

Atomically precise synthesis is still beyond reach for colloidal semiconductor NCs, despite promising recent advances for CdSe QDs,[15,16] but is nonetheless already routinely carried out for a class of materials known as magic-size clusters (MSCs). The term magic-size cluster is used to denote atomically precise clusters of metals or semiconductors characterized by a well-defined number of atoms and higher stability than slightly larger or smaller clusters.[18,19] MSCs of semiconductors have been implicated as intermediates in the formation of colloidal NCs through nonclassical nucleation and growth pathways.[18−22] However, for reasons to be discussed in more detail below, their exact role is still under intense debate, as it seems to vary depending on the system conditions, resulting in conflicting reports.[18−20] Furthermore, the stability and growth mechanisms of semiconductor MSCs are still poorly understood, despite several decades of extensive research. MSCs grow in a discontinuous and quantized fashion, in discrete jumps from one magic size to the next, without the appearance of intermediate sizes, in striking contrast with the continuous growth regime typically observed for colloidal semiconductor NCs.[18−20,23]

Interestingly, the confinement dimension (i.e., diameter or thickness) of ultrathin colloidal nanowires, nanoribbons, nanoplatelets, and nanosheets also increases in discrete steps, even though these NCs are not atomically precise.[4,24] We thus propose that ultrathin (smallest dimension ≤2 nm) 1D and 2D NCs can be categorized as magic-size nanocrystals (MSNCs), as their critical dimension (diameter or thickness, respectively) is atomically precise and changes only in discrete steps. The magic-size regime is typically taken to extend from a few atoms up to a few tens of atoms (∼2 nm), after which the continuous growth regime is entered.[18−20] However, the notion that quantized growth is restricted to the cluster-size regime has been recently challenged by reports demonstrating discrete growth of CdSe well into the size range of colloidal QDs (i.e., up to 3.5 nm).[15,16,25] This observation, in combination with the insight discussed above that ultrathin 1D and 2D NCs can be regarded as magic-size nanocrystals, raises several intriguing questions: Are the formation mechanisms leading to magic-size clusters and magic-size nanocrystals (regardless of their dimensionality) fundamentally the same? And how does the formation mechanism of magic-size species differ from that leading to the continuous growth regime observed for conventional colloidal NCs? These questions have been recently partially addressed by Norris and co-workers for the specific case of zinc blende CdSe QDs and nanoplatelets.[15] In this Perspective, we intend to further discuss these points. To this end, we will critically analyze the currently available knowledge on the formation and stability of both MSCs and MSNCs (0D, 1D, and 2D). We will then use the insights gained in our analysis to propose a unified view of the formation and quantized growth of magic-size species. Considering that clusters are distinctly different from nanocrystals, as they are too small to possess long-range periodicity, we will use the term magic-size nanostructures (MSNSs) to encompass both MSCs and MSNCs. This term will also be used when the exact nature of the magic-size species is unknown or uncertain. This Perspective is intended as a concise and critical assessment of the state-of-the-art, in which the outstanding challenges are identified and highlighted. For further details, the interested reader is referred to several recent

https://doi.org/10.1021/acsmaterialsau.1c00075
ACS Mater. Au 2022, 2, 237−249

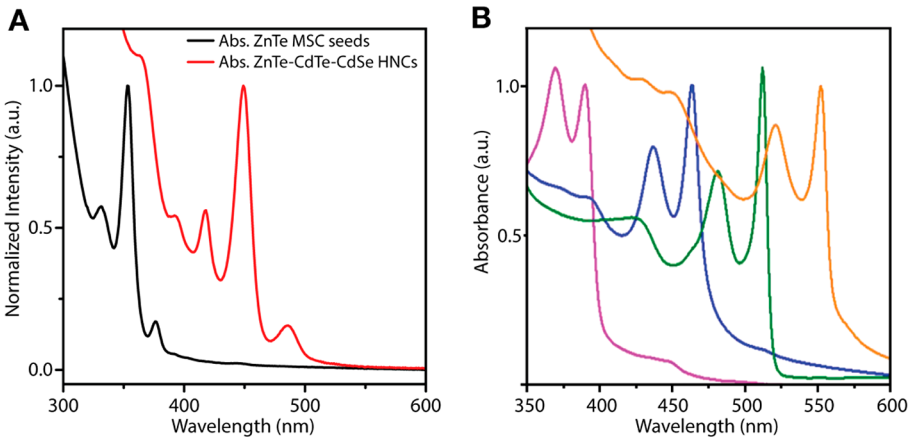

Figure 2. (A) Absorption spectra of ZnTe MSCs (black curve) and ultrathin (2 nm diameter) (Zn,Cd)Te/CdSe heteronanowires (red curve). Adapted from ref 26. Copyright 2012 American Chemical Society. (B) Absorption spectra of ultrathin CdSe nanoplatelets of different thicknesses (0.8, 1.1, 1.4, and 1.7 nm, from left to right, respectively). Adapted from ref 24. Copyright 2016 American Chemical Society.

reviews focusing on different aspects of MSCs and colloidal 1D and 2D NCs.[4,18−20,23,24]

2. ZERO-DIMENSIONAL MAGIC: ATOMICALLY PRECISE SEMICONDUCTOR CLUSTERS

2.1. The Challenge of Unambiguous Identification of Magic-Size Clusters

Advances in the understanding of the fundamental principles governing the quantized growth of MSCs and their higher (meta)stability have been hindered by the lack of accessible characterization tools capable of reliably and accurately probing MSCs in their native environment (i.e., dispersed in liquid media) at the very small sizes that typify them (≤2 nm) and at relevant temperatures and time scales. The opportunities and challenges regarding the characterization of MSCs have been recently reviewed by Palencia et al.,[18] who concluded that the combination of different techniques and the use of in situ characterization tools such as optical spectroscopy, small-angle X-ray scattering (SAXS), extended X-ray absorption fine structure (EXAFS), and pair distribution function (PDF) analysis is indispensable. They further argue that in situ optical spectroscopy is one of the most promising tools because MSCs are characterized by very narrow absorption peaks, which red shift in discrete steps as the MSCs grow.[18] Given that the exact composition and structure of MSCs is rarely known, this reasoning has led to the widespread practice of referring to MSCs by their lowest energy absorption transition, for example, CdSe-418 for a CdSe MSC displaying a band edge absorption peak at 418 nm. As a result, MSCs are typically identified solely based on their absorption spectra, often using the observation of quantized growth to support the assignment. We would like here to strongly caution against this practice, as sharp and discrete absorption transitions are also spectral signatures of ultrathin 1D and 2D NCs (Figure 2). Further, as we will discuss in more detail below (section 3), spectral changes do not necessarily reflect a change in the MSC size as they may also be induced by changes in surface chemistry, isomerization, or conversion of MSCs into other MSNSs such as nanowires and nanosheets. It is thus possible that the similarity of the absorption spectra of MSCs and ultrathin 1D and 2D MSNCs has led to the misidentification of the absorbing species in reports employing absorption spectroscopy as the sole characterization technique.

The use of multiple techniques is thus essential to allow a reliable distinction between different MSNSs. However, combining different characterization techniques does not necessarily ensure unambiguous assignments. For example, mass spectrometry has been often employed to determine the composition of MSCs (e.g., $(CdSe)_{34}$),[18,20,27−29] but its accuracy and reliability have been questioned by several groups because the same mass fragments can be observed from colloidal QDs (regardless of their size) or from the bulk material upon laser ablation,[16,30] suggesting that they are merely the most stable fragments of II−VI semiconductors in the gas phase. Furthermore, mass spectrometry is not always conclusive due to heavy fragmentation of the MSNSs originally present in solution.[18,28,31] It is also plausible that the composition of the species observed in the mass spectra reflects the stability of bare clusters in the gas phase, being thus unrelated to that of the original MSCs in solution.[18] We thus advocate the use of transmission electron microscopy (TEM) as a companion characterization technique to lift ambiguities in assignments based on absorption spectroscopy, as it allows for straightforward distinction between 1D and 2D MSNCs and MSCs (even if only because the latter are typically too small to be clearly observed in conventional TE microscopes). TEM is often deemed inadequate for this purpose due to the weak contrast, poor resolution, and high e-beam sensitivity of MSCs owing to their small size.[18] Moreover, drying and aggregation effects may make the interpretation of the images difficult.[18] We acknowledge these challenges but argue that they may be mitigated by a judicious work protocol and the use of advanced instruments allowing lower e-beam doses. Furthermore, recent advances in the field of high-resolution cryo-TEM make it possible to image the MSNSs directly in their native environment.

The composition and structure of MSCs is known for only a few cases. Nevertheless, there is evidence that the ligands bound to the MSCs have a decisive impact on their stoichiometry, structure, and stability.[18−20] X- and Z-type ligands (i.e., negatively charged electron-pair donors such as carboxylates and metal−ligand complexes, respectively) lead to nonstoichiometric MSCs, likely due to charge neutrality requirements.[18−20,32] In contrast, neutral L-type electron pair donors (such as amines and phosphines) seem to favor stoichiometric II−VI MSCs, although the exact structures of

https://doi.org/10.1021/acsmaterialsau.1c00075
ACS Mater. Au 2022, 2, 237−249

these species remain elusive.[18,20,32] Considering the very high surface to volume ratio of MSCs and the hybrid organic–inorganic nature of colloidal semiconductor NCs, in general,[1] the crucial importance of the ligand capping layer is not surprising. However, the mechanisms through which the ligand influence is exerted have not yet been fully elucidated.

2.2. Nonstoichiometric Magic-Size Clusters

Nonstoichiometric clusters of II–VI semiconductors (II = Cd, Zn; VI = S, Se, Te) with charged X-type ligands (carboxylates and selenolates) have been extensively studied in the past decades. The CdSe congeners are particularly well-characterized and were shown already in the early 1980s[33] to consist of a homologous series of tetrahedral clusters built of either pure adamantane cages or mixed adamantane and barylene cages (Figure 3).[34] These structural units are both based on

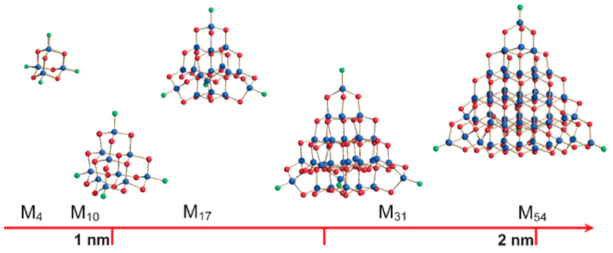

Figure 3. Schematic representation of the structure of II–VI MSCs determined by single-crystal XRD. The clusters are built of either pure adamantane cages or mixed adamantane and barylene cages, the building blocks of the zinc blende and wurtzite structures of II–VI semiconductors, respectively. The axis indicates the equivalent diameter (defined as the tetrahedron height). M_4 = $[M_4(ER)_6L_4]^{2-}$ (0.4 nm), M_{10} = $[M_{10}E_4(ER)_{12}L_4]$ (0.7 nm), M_{17} = $[M_{17}E_4(ER)_{24}L_4]^{2+}$ (1.0 nm), M_{31} = $[M_{32}E_{14}(ER)_{36}L_4]$ (1.5 nm), and M_{54} = $[M_{54}E_{32}(ER)_{48}L_4]^{4-}$ (2.0 nm) (M = Cd, Zn, blue dots; E = S, Se, Te, red dots; L = two electron ligand at the tetrahedral apical sites, typically tertiary phosphines or water, green dots; R = alkyl or aryl groups, not shown). Reproduced with permission from ref 34. Copyright 2009 Wiley-VCH GmbH.

tetrahedrally coordinated metal and chalcogen atoms but differ in the way the tetrahedra are connected, leading to cubic close packing for the adamantane cages and hexagonal close packing for the barylene cages. It is interesting to note that adamantane and barylene cages are the building blocks of, respectively, the zinc blende and wurtzite structures of bulk II–VI semiconductors, implying that nonstoichiometric II–VI MSCs can be seen as well-defined fragments of the bulk materials stabilized by ligands.[34] These early findings were later corroborated by other studies,[16,35,36] which demonstrated that nonstoichiometric II–VI MSCs consistently adopt structures and shapes like those shown in Figure 3, regardless of their exact composition (*i.e.*, Se-rich or Cd-rich). For example, Owen and co-workers recently synthesized a series of Cd-rich CdSe clusters of composition $Cd_{35}Se_{20}(X)_{30}(L)_{30}$, $Cd_{56}Se_{35}(X)_{42}(L)_{42}$ and $Cd_{84}Se_{56}(X)_{56}(L)_{56}$ (X = O_2CPh, L = $H_2N-C_4H_9$), which were shown by single-crystal X-ray diffraction (XRD) and atomic PDF analysis to consist of a series of tetrahedral clusters with Cd-terminated {111} facets (sizes: 1.71, 2.14, and 2.57 nm, respectively).[16] Metal-rich II–VI MSCs have been isolated as solids also in other studies,[30,37] but structural determination has been rarely done. In most cases, the assignment of the observed species to MSCs is based solely on the similarity of their absorption spectra to previously published results. However, as discussed above (section 2.1), this practice may lead to misinterpretation of the data, as it is based on assumptions that are not necessarily valid. Although the majority of the studies address II–VI MSCs, well-characterized metal-rich MSCs capped by X-type ligands have also been obtained for InP (e.g., $In_{37}P_{20}(O_2CR)_{51}$).[38,39] In contrast to II–VI MSCs, the structure of InP MSCs deviates from that of known crystal phases, consisting of a non-stoichiometric charged core composed of a series of fused six-membered rings.[38]

2.3. Stoichiometric Magic-Size Clusters

To date, stoichiometric MSCs have been reported only for II–VI semiconductors and exclusively in the presence of L-type ligands (alkylamines).[20] Unfortunately, efforts to isolate them as solids suitable for single-crystal XRD analysis have so far been unsuccessful, typically yielding alkylamine-based lamellar mesostructures in which the MSCs are (presumably) entrained.[20,21,27−29] As a result, the structures of this class of MSNSs remain unknown, although theoretical calculations suggest that stoichiometric II–VI MSCs should have cage-like structures (Figure 4).[29,40] Their composition has been

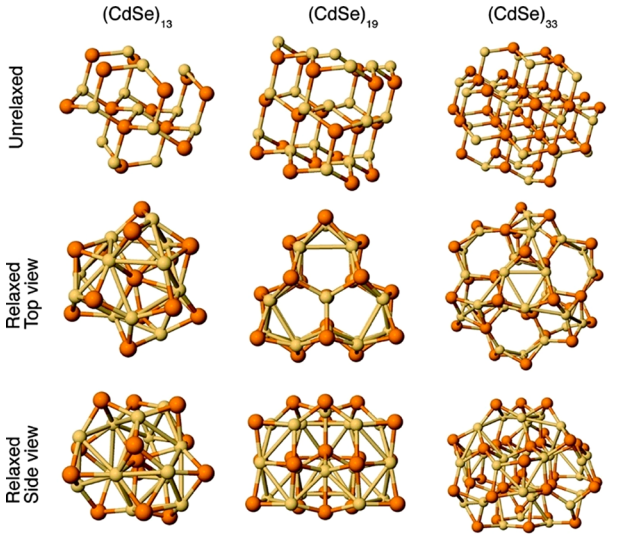

Figure 4. Structures of unrelaxed and relaxed wurtzite $(CdSe)_n$ clusters (n = 13, 19, and 33) calculated by time-dependent density functional theory. Ligands are omitted for clarity but were included in the calculation using ammonia and methyl amine as models for amines and formic and acetic acids as models for fatty acids. The side view is parallel to the *c*-axis; the top view is along the *c*-axis (Cd and Se are represented by yellow and bronze spheres, respectively). Reproduced from ref 40. Copyright 2011 American Chemical Society.

deduced solely using a combination of elemental analysis of the isolated solids (which yields empirical formulas) and mass spectrometry (MS) studies.[20,21,27−29] Surprisingly, the stoichiometric clusters detected by MS have always been devoid of any ligands.[18,20] Moreover, as discussed above (section 2.1), the reliability of the compositions determined by MS has been called into question by several groups.[16,30] This is consistent with the observation that there seems to be an upper limit to the cluster size that can be identified by MS, as only $(ME)_{13}$, $(ME)_{19}$, and $(ME)_{34}$ have been observed by analysis of both colloidal MSCs[20,21,29] and bulk materials.[29,41] Interestingly, the UV–visible spectra theoretically calculated by Del Ben et al.[40] for stoichiometric CdSe MSCs assuming the theoretically

https://doi.org/10.1021/acsmaterialsau.1c00075
ACS Mater. Au 2022, 2, 237–249

determined cage-like structures (Figure 4) are in good agreement with the experimental ones published for non-stoichiometric CdSe MSCs by Kudera et al.[30] It has been pointed out that the absorption features of some non-stoichiometric CdSe MSCs match exactly those of stoichiometric CdSe MSCs with fewer units.[20,28] These observations are intriguing as the structure of stochiometric and non-stoichiometric MSCs are expected to be very different (viz., adamantane/barylene tetrahedral frameworks, Figure 3, and fullerene-like cages, Figure 4). Further, theoretical[40] and experimental[42,43] results have demonstrated that the ligands have a crucial impact on the optical gap of the clusters. It is therefore likely that the agreement between the absorption spectra of stoichiometric and nonstoichiometric MSCs is fortuitous, calling for more detailed theoretical and experimental investigations of the geometry and electronic structure of these MSNSs.

From this standpoint, the study recently published by Hsieh and co-workers[44] is of particular interest. The authors used a combination of nondestructive characterization techniques (TEM, SAXS, wide-angle X-ray scattering (WAXS), EXAFS, XRD, X-ray photoelectron spectroscopy, magic-angle spinning NMR spectroscopy) and computational approaches to study the shape, size, local bonding, and chemical environments of octylamine-capped MSNSs that have been previously[28] assigned to $(CdSe)_{13}$ MSCs.[44] The isolated solids are observed to consist of 1.6 nm diameter clusters entrained into self-assembled sheet-like triangular lamellae.[44] We note that the observed diameter is much larger than that expected for $(CdSe)_{13}$ MSCs (~0.7 nm). Ligand exchange of octylamine by oleylamine, followed by repeated dilution and sonication yielded clear solutions that were shown to contain paired ellipsoidal clusters with two radii (8.5 and 8.1 Å).[44] This configuration was supported by computational approaches which suggested that the spontaneous pairing of the clusters was driven by strong dipole−dipole interactions. These interactions were also proposed to induce the self-organization of the paired clusters into stripped 2D superlattices, consistent with the experimental observations.[44] This study suggests that the structure of stoichiometric II−VI MSCs is fundamentally different from that of nonstoichiometric II−VI MSCs and implies that the former are not present as independent species. The latter point reinforces our recommendation above (section 2.1) that caution should be exercised when drawing conclusions based only on absorption spectroscopy. Nevertheless, the generality of these observations for other stoichiometric II−VI MSCs remains to be demonstrated.

2.4. Current Insights in the Formation and Stability of Magic-Size Clusters

MSCs have been rationalized in terms of nonclassical nucleation models, in which each subsequent MSC size occupies a local free energy minimum in the progression from precursors to nanocrystals (Figure 5).[19,20,45−47] Their characteristic quantized growth pathways are thus interpreted as discrete jumps from one minimum to the next. In most cases, MSCs have not been isolated but were identified through their spectral signatures during the synthesis of colloidal II−VI, IV−VI, and III−V nanocrystals.[19] Their presence is often transient and restricted to the early stages of the synthesis, leading to the notion that MSCs are kinetically persistent intermediates which can either grow further to regular nanocrystals or redissolve, acting as monomer reservoirs.[19] A recent in situ SAXS and optical spectroscopic study of the formation of CdSe nanocrystals from Cd-octadecylphosphonate (Cd-ODPA) and trioctylphosphine-Se (TOP-Se) has shown that these different scenarios are not mutually exclusive and that CdSe MSCs are formed at all temperatures investigated (260−330 °C).[46] Quantized growth of $(CdSe)_n$ (n = 13, 19, 33, 66, and 84) MSCs persists for a longer time and reaches larger n values at lower temperatures, whereas at higher temperatures, the system transitions into the continuous growth regime faster, before larger MSC sizes are reached.[46] This is consistent with the view that MSCs are kinetically trapped products and that the energy barriers for growth progressively decrease as MSCs become larger. The study also showed that MSCs can both grow directly to NCs by monomer addition or redissolve to provide monomers for NC growth, depending on the temperature and reaction time.[46] These observations were rationalized by a monomer-driven growth mechanism governing both quantized and continuous growth regimes and kinetically limited by temperature-dependent monomer formation rates.[46] The quantized and continuous growth regimes were proposed to be kinetically coupled also through a temperature-dependent MSC formation and dissolution equilibrium.[46]

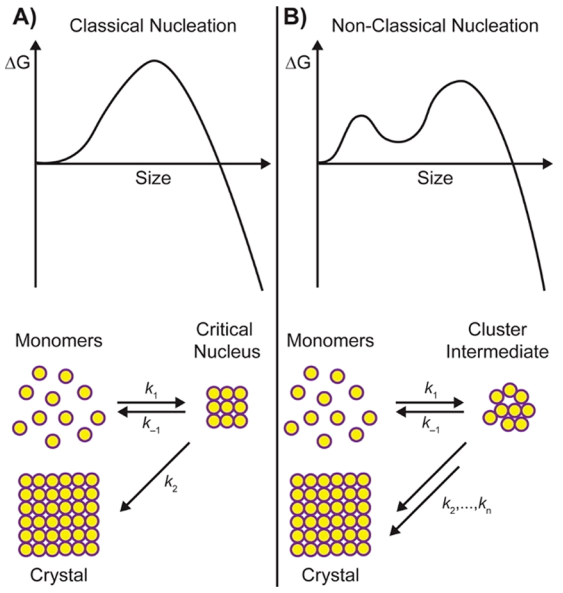

Figure 5. Free energy change as a function of particle size and schematic representations of the crystallization process for (A) classical and (B) nonclassical nucleation models. Reproduced from ref 47. Copyright 2016 American Chemical Society.

The crucial role of the reaction temperature in the formation and stability of MSCs has been previously demonstrated in many studies and is best illustrated by the fact that MSCs are most often observed at low temperatures (<100 °C)[19,20,45,48] and have only been isolated as solids suitable for structural analysis at temperatures close to room temperature or below.[16,33,35,36] This implies that the energy barriers locking MSCs in their preferred configurations and hindering their growth in a continuous fashion are rather small. Intriguingly, the resistance of MSCs to thermally induced growth (i.e., their thermal stability) is strongly dependent on the nature of the ligands present.[19] For example, the thermal stability of CdSe MSCs ranges from room temperature for alkylamine ligands[21,45] to ~100 °C for a mixture of alkylcarboxylate and

https://doi.org/10.1021/acsmaterialsau.1c00075
ACS Mater. Au 2022, 2, 237−249

alkylamine ligands[30] to as high as 300 °C for alkylphosphonate ligands.[46,49] Interestingly, despite the high thermal stability of CdSe MSCs with phosphonate ligands, their formation is precluded upon addition of alkylamines, which promote continuous growth instead.[50] Similar observations have been reported for MSCs of other II−VI semiconductors and of InP.[19] Moreover, shorter chain ligands have been reported to yield CdSe MSCs absorbing at higher energies, leading to the conclusion that the ligand chain length affects the size of the MSCs, under the assumption that the MSCs were 0D nanostructures and that their absorption energies were entirely dictated by their sizes.[19] Although reasonable, this assumption has not been verified, and it is thus possible that the species responsible for the absorption transitions were in fact not 0D. For example, the most persistent CdSe MSCs observed at the early stages of the synthesis of CdSe nanorods from Cd-ODPA and TOP-Se are characterized by an intense absorption maximum at 350 nm and are believed to be molecularly well-defined tetrahedral clusters of zinc blende CdSe.[49] However, a recent work has demonstrated that this characteristic absorption spectrum originates from ultrathin (1.9 nm diameter) 1D fibrillar nanostructures of empirical formula $[(CdSe)_{13}(CdODPA)_{13}(ODPA)_{32}]$ that form at the early stages of the above-mentioned synthesis.[50]

The observations discussed above imply that the (meta)-stability of MSCs is largely determined by the ligands. However, the exact role of ligands on the formation and stabilization of MSCs remains unclear and likely depends on the interplay between ligands, precursors, and other adjuvant chemicals present in the reaction medium, as well as on the temperature, concentration of ligands, and nature of the solvents used. Several lines of evidence support the view that the impact of ligands is multifaceted, encompassing modulation of precursor reactivities and monomer solubility,[19] alteration of reaction pathways,[19] formation of preferred metastable configurations,[37] and stabilization through mesophases.[20,21,51] It has been suggested that ligands increase monomer solubility and precursor reactivity, thereby facilitating the high oversaturations required for the formation of MSCs.[19] This argument is supported by the fact that syntheses employing highly reactive precursors and high concentrations favor MSC formation, especially if the constituent elements of the MSC are already in their final oxidation state in the precursors (e.g., Cd^{2+} and Se^{2-} for CdSe MSCs).[19,25,52] However, the observation that the formation of ZnTe MSCs from diethylzinc and trioctylphosphine tellurium is promoted by primary alkylamines but suppressed by tertiary alkylamines under otherwise identical conditions implies that the ligands have a direct impact on the stability of the MSCs,[37] either by favoring a particular configuration with a higher thermodynamic stability or by restricting access to the MSCs, thereby kinetically stabilizing preferred sizes or conformations. This inference is further supported by reports showing the interconversion between different types of CdE MSNSs (E = S, Se, Te) upon increasing the concentration of alkylamines in solution[45,53−55] or upon adsorption−desorption of OH groups in the solid state[42] (see section 3 below).

Based on the observation by room temperature XRD and TEM of lamellar structures in samples that display the characteristic spectral signatures of CdSe MSCs, some authors have proposed that the formation of stoichiometric II−VI MSCs proceeds via lamellar mesophase templates.[20,21,29] However, the fact that such mesophases have been observed by SAXS to melt at temperatures below those at which the MSCs and MSNSs were synthesized or observed[46,56,57] has led others to question the validity of this formation mechanism. This view has been reinforced by a recent work showing that the $[(CdSe)_n(alkylamine)_m]$ lamellar mesophases observed at room temperature in previous studies[21] are likely a reaction product because the intensity of their SAXS pattern collected ex situ at room temperature increased continuously during the reaction, closely following the increase in the intensity of the WAXS and optical absorption signals attributed to CdSe MSCs.[44]

Further insight into the role of mesophases has been recently provided by a study of the formation of CdS MSCs from Cd-oleate and trioctylphosphine sulfide at 130 °C.[51] The study reports that the formation of CdS MSCs is promoted by high precursor concentration (1000 mM) and is accompanied by the formation of a hexagonal organic−inorganic mesophase, as evidenced by in situ SAXS/WAXS at the reaction temperature (Figure 6A,B).[51] Scanning transmission electron microscopy

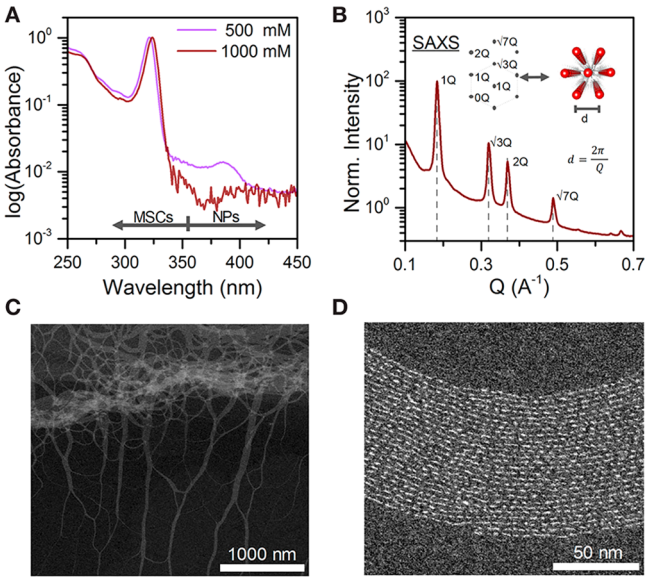

Figure 6. (A) Absorption spectra of cleaned CdS MSCs prepared at two different metal precursor concentrations (500 and 1000 mM). (B) In situ SAXS of 1000 mM CdS MSC synthesis at 6 h at 130 °C. Inset: Reciprocal and real space model of hexagonal MSC assembly. (C,D) STEM images of cleaned CdS MSCs. (C) Long (>1 μm) bundles of fibers composed of MSCs. (D) Zoomed-in view of the fibers shown in C. Adapted from ref 51. Copyright 2018 American Chemical Society.

(STEM) images of the samples diluted in toluene showed long bundles of fibrils, which upon zoom-in appeared to consist of strings of discrete inorganic entities of ∼1−2 nm (Figure 6C,D).[51] We note that it remains to be investigated whether the segmentation has been induced by e-beam damage, as the authors of the study acknowledged that the clusters degraded quickly under electron irradiation. The mesophase also formed at intermediate precursor concentration (500 mM) but progressively disappeared after 2 h, while QDs formed (Figure 6A).[51] At 100 mM, mesophase peaks were not observed and MSCs were not obtained.[51] The authors of the study proposed that the resistance of the MSCs to growth and dissolution (i.e., their improved stability) arises from their embedding into fibrous mesophase assemblies that self-assemble at sufficiently

https://doi.org/10.1021/acsmaterialsau.1c00075
ACS Mater. Au 2022, 2, 237−249

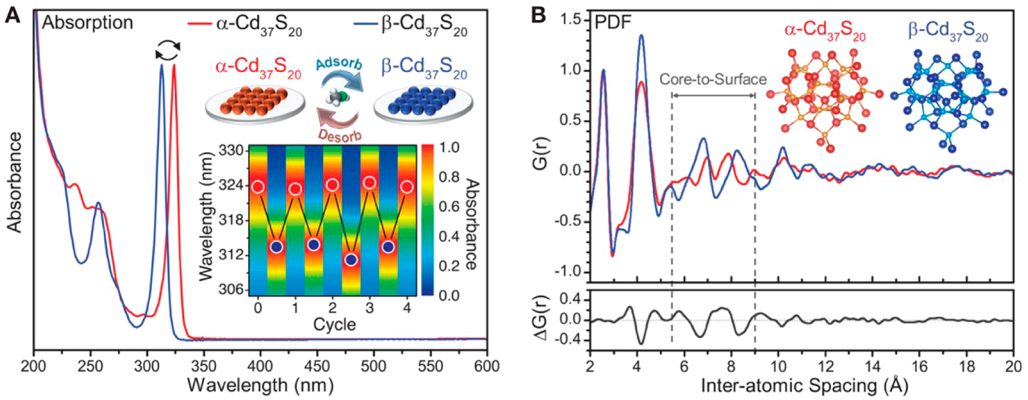

Figure 7. (A) Absorption spectra of pristine cluster isomers α-$Cd_{37}S_{20}$ and β-$Cd_{37}S_{20}$, with excitonic peaks at 324 and 313 nm, respectively. The two isomers switch reversibly upon alcohol adsorption and desorption (inset schematic and contour plot). The slight deviation between cycles is associated with ambient temperature fluctuations. (B) PDFs of the α and β isomers. $\Delta G(r) = G_\alpha(r) - G_\beta(r)$ is the difference in the PDF between the two isomers and is largest for core-to-surface atom pair distances. Inset are the fitted structures of the α and β isomers with residuals of ~0.18. Reprinted with permission from ref 42. Copyright 2019 AAAS.

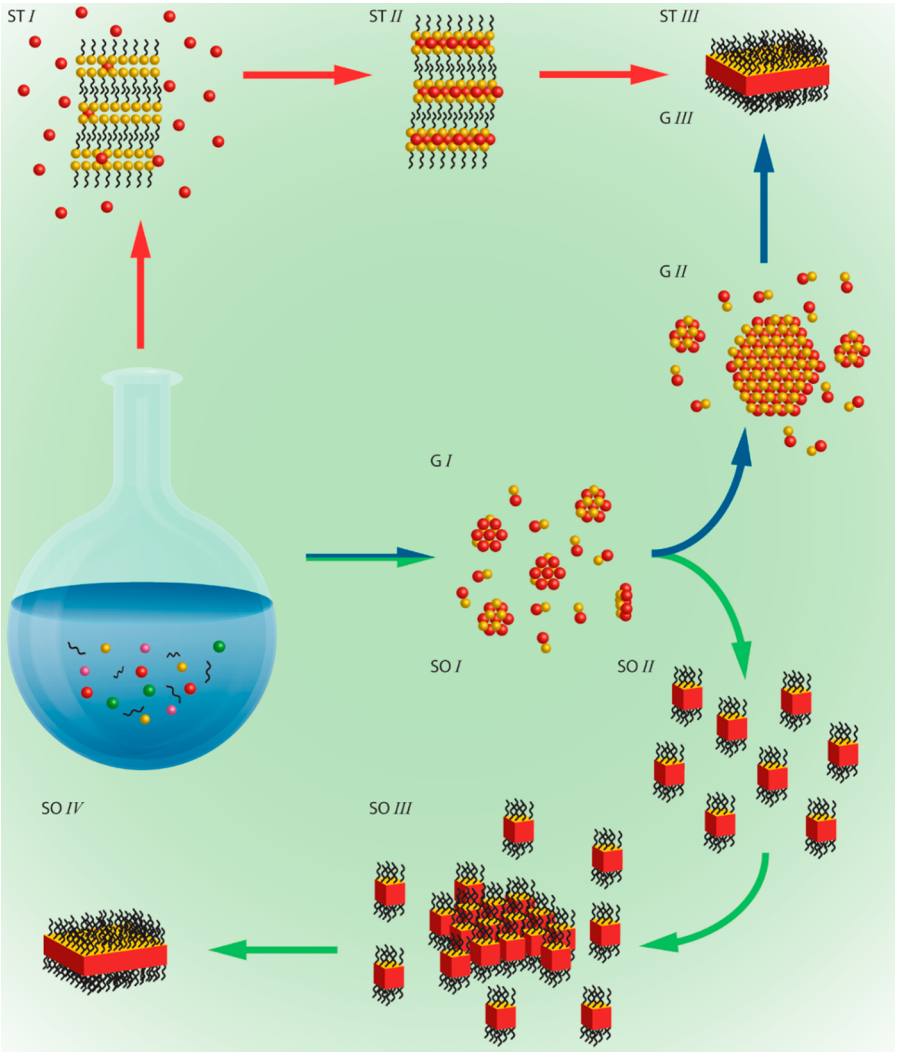

Figure 8. Schematic overview of formation mechanisms for ultrathin 2D NCs. The pathway indicated with red arrows shows the soft template (ST) mechanism, in which the template (ST *I*) imposes 2D constraints to either the nucleation and growth or the oriented attachment of MSCs (ST *II*). The pathway indicated with blue arrows shows the 2D-constrained kinetics mechanism (G), in which MSC seeds (G *I*) grow only in the lateral direction (G *II*). The pathway indicated by green arrows illustrates NS formation through 2D self-organization (SO). Nucleation (SO *I*) and growth of NC building blocks (SO *II*) are followed by self-organization (SO *III*) and oriented attachment (SO *IV*). Reproduced from ref 4. Copyright 2017 American Chemical Society.

https://doi.org/10.1021/acsmaterialsau.1c00075
ACS Mater. Au 2022, 2, 237−249

high supersaturations of both surfactants (ligands) and inorganic species, effectively shielding the MSC nuclei from the reaction medium, thus suppressing their growth.[51] The switch from quantized to continuous growth was thus attributed to conditions that destabilize the mesophase, such as higher temperatures, lower concentrations, or addition of coordinating ligands (e.g., trioctylphosphine oxide or oleylamine).[51] Interestingly, the self-assembly of the fibrillar organic−inorganic mesophases seems to be driven primarily by the inorganic MSC core, as identical fibrils were obtained regardless of the precursor chain length.[51] In our view, this implies that the mesophase is not acting as a template but instead synergistically interacts with the MSCs as they nucleate to promote a reaction pathway that kinetically favors the formation of hybrid organic−inorganic 1D fibrils.

3. INTERCONVERSION BETWEEN MAGIC-SIZE NANOSTRUCTURES

Transformation of MSNSs evidenced by spectral changes has been reported by several groups. Kasuya and co-workers[53] observed that octylamine-capped CdSe MSNSs absorbing at 415 nm, previously assigned to $(CdSe)_{34}$ MSCs,[29] were converted to MSNSs absorbing at 350 nm by increasing the concentration of octylamine in a solution in toluene at room temperature. The transformation led to the formation of a precipitate, which was shown to consist of lamellar structures, presumed to consist of MSCs with 1.2 nm diameter.[53] Similar spectral transformations were recently reported by Buhro and co-workers for alkylamine derivatives of stoichiometric ZnSe, CdSe, and CdTe MSNSs and interpreted as conversion of $(ME)_{34}$ MSCs to $(ME)_{13}$ MSCs.[28] The transformation process was significantly accelerated in mixtures rich in a primary alkylamine.[28] The assignment of the starting and final species to $(ME)_{34}$ MSCs and $(ME)_{13}$ MSCs was done primarily on the basis of absorption spectra, by analogy with spectra that had been previously assigned to those species.[28]

Transformations involving II−VI (CdS, CdSe, CdTe) MSNSs in colloidal dispersion have been extensively investigated by Yu and co-workers,[45,54] who reported that the absorbance of the original species continuously decreased while that of the final species increased. The spectral transformations were induced by changes in the concentration of alkylamines (e.g., CdTe MSCs) and/or temperature (e.g., CdS MSCs) and were attributed to interconversion between different MSCs through postulated intermediates presumed to constitute a group of quasi-isomers.[45,54] Nevertheless, the interconversions were followed only by absorption spectroscopy, and therefore, the nature of the involved MSNSs remains unclear. Direct observation of interconversion between MSCs has been recently reported by Robinson and co-workers, who demonstrated that solid-state $Cd_{37}S_{20}$ MSCs undergo reversible isomerization between two discrete and stable states through a chemically induced reconfiguration of the inorganic core (Figure 7).[42] The switching between the isomers is triggered by the adsorption−desorption of OH groups and is accompanied by a 140 meV spectral shift.[42] It is plausible that similar isomerization processes could explain the transformations previously observed by other groups for MSNSs in solution (see above), but other processes such as changes in dimensionality (e.g., conversion from 0D MSCs to 1D nanowires or 2D nanosheets; see below) are also likely and cannot be excluded, especially in cases where the transformations are not reversible.

4. ONE- AND TWO-DIMENSIONAL MAGIC: ULTRATHIN NANOWIRES AND NANOSHEETS

Colloidal ultrathin 2D semiconductor MSNCs, such as nanoribbons (NRBs), nanoplatelets (NPLs), and nanosheets (NSs), have been extensively investigated over the past decade.[4,24] Nevertheless, despite this intense research activity, there is still no consensus in the scientific community regarding their formation mechanism, as several possibilities have been proposed (Figure 8).[4] These different mechanisms are all supported by evidence but remain nonetheless under discussion because experiments supporting one of them typically cast doubt on competing mechanisms. The debate regarding their validity is thus based on the idea that the different mechanisms are mutually exclusive. To assess the validity of this assumption, we will briefly address below the evidence supporting each of the mechanisms depicted in Figure 8.

The soft template mechanism (Figure 8, ST) has been shown by in situ SAXS to be operative in the formation of ultrathin $Cu_{2-x}S$ NSs, in which 2D mesophases constrain the nucleation and growth of $Cu_{2-x}S$ NCs upon thermolysis of Cu-thiolate frameworks.[58] The template mechanism has also been used to explain the formation of wurtzite CdSe NRBs, NPLs, and NSs.[21] In this case, the formation of 2D MSNCs is assumed to proceed through self-assembly of MSCs entrained in a 2D bilayer mesophase template. The existence of these lamellar templates has been evidenced at room temperature by low-angle XRD[21] but has yet to be verified at the reaction temperatures (typically 50−120 °C). The formation of 2D MSNCs through template-free 2D-constrained self-assembly of building blocks has also been proposed (Figure 8, SO).[4,59] For example, the formation of PbS NSs has been ascribed to 2D-oriented attachment of PbS NCs, in which the 2D constraint was attributed to a dense and highly ordered oleic acid layer selectively capping the (100) facets.[60] A similar mechanism has been proposed for the formation of covellite In-poor $CuIn_xS_2$ NSs.[61]

Interestingly, the formation of ultrathin 2D zinc blende CdX (X = S, Se, Te) NPLs has been explained by mechanisms that do not require templates or oriented attachment, relying instead on 2D growth kinetic instabilities (Figure 8, G).[15,24] It has been demonstrated that in the case of zinc blende CdX NPLs, mesophases that could act as templates are absent at the growth temperatures, even in reactions carried out in molten Cd-carboxylates.[15] In the 2D-constrained kinetics mechanism, the 2D growth anisotropy is attributed to a much larger activation energy for island nucleation on the top and bottom large planar facets with respect to the narrow side facets, as these are smaller than the critical 2D island size for nucleation.[15] Under the assumption that the 2D nucleation is the rate-limiting step, this leads to much smaller kinetic barriers for growth on the thin side facets than on the large top and bottom facets, provided the local concentration of precursors is sufficiently high to sustain surface-reaction-limited growth.[15] The enhanced growth rates of the narrow facets would then lead to an intrinsic instability that drives 2D NPL formation.

The formation of ultrathin 1D MSNCs has been much less investigated compared to that of their 2D counterparts and is almost exclusively ascribed to oriented attachment of MSCs.[4] This mechanism has been supported by the observation of strings of interconnected particles at early stages of the growth,

https://doi.org/10.1021/acsmaterialsau.1c00075
ACS Mater. Au 2022, 2, 237−249

prior to their fusion into single-crystalline wires.[4,59] The 1D self-organization process is typically assumed to be driven by dipolar interactions between the building blocks.[4,59] This assumption, however, has yet to be experimentally validated. Moreover, the role of ligands in the formation of 1D MSNCs remains unclear. It has been suggested that ligands could play a decisive role in 1D-oriented attachment by selectively exposing certain facets and/or inducing dipolar interactions due to asymmetric distribution of dissimilar ligands.[4] It is also possible that van der Waals interactions confer additional stability to 1D MSNCs, as ligands containing linear alkyl chains are typically needed to obtain these nanostructures.[4]

We note that ligands play a crucial role in both the 2D soft template and the 2D-oriented attachment mechanisms, but in the latter, their 2D directive effect is exerted through a synergistic interaction that occurs concurrently with the growth of the 2D NCs, in contrast with the former, which requires the template to form prior to the onset of 2D growth. Although the 2D-constrained growth kinetics mechanism discussed in ref 15 does not require the involvement of ligands, it does not necessarily exclude the possibility that ligands have an adjuvant role, amplifying kinetic imbalances by increasing the stability of the top and bottom flat facets, as these facets allow the assembly of dense ligand monolayers stabilized by van der Waals interactions.[4]

Based on the observations discussed above, we can conclude that the notion of a single mechanism capable of accounting for the formation of all types of ultrathin 1D and 2D MSNCs is unsubstantiated. Moreover, this view is incompatible with the fact that these systems represent metastable states in a multidimensional variable space and as a result may be accessed through different pathways. It is thus conceivable that different formation mechanisms coexist, interacting dynamically in a synergistic or antagonistic way, depending on the physical−chemical conditions prevailing during the synthesis. This scenario is consistent with recent experimental observations and will be discussed in more detail in the next section.

5. CORRELATIONS BETWEEN QUANTIZED GROWTH PATHWAYS OF 0D, 1D, AND 2D MAGIC-SIZE SEMICONDUCTOR NANOSTRUCTURES

As previously pointed out in ref 4, the precursors and synthetic protocols used to obtain ultrathin 2D, 1D, and 0D colloidal MSNSs of II−VI semiconductors are remarkably similar, differing mainly regarding the reaction temperatures, which are typically higher for 1D NWs than for 2D NSs (viz., 100−180 and 25−100 °C, respectively). This observation was taken in ref 4 to suggest that the dimensionality of the MSNSs is determined primarily by the reaction temperature. Considering the large body of evidence implying that ligands play decisive roles in the formation of MSNSs, it was then proposed that the dimensionality of the resulting MSNSs was dictated by the thermal stability of the soft templates formed by the ligands.[4] Given the short-range and weak nature of van der Waals interactions between alkyl chains, thermal fluctuations should easily disrupt the long-range in-plane order of 2D templates formed by self-organization of ligand molecules, favoring the formation of 1D superstructures stabilized by both dipolar interactions between the inorganic building blocks and van der Waals interactions between densely packed ligands organized in a tubular array (Figure 9). At even higher reaction temperatures, 1D templates would also destabilize, favoring 0D structures (Figure 9). We note that this model is also valid

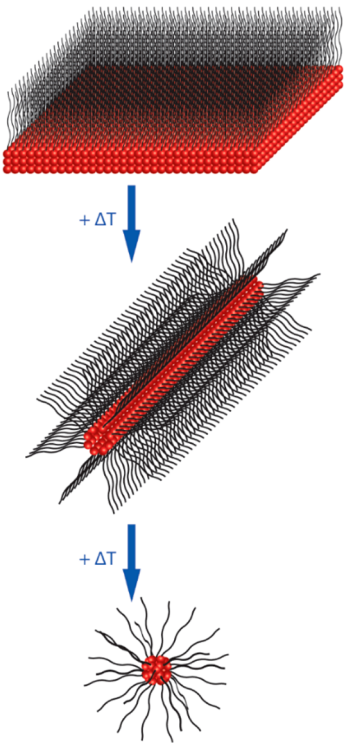

Figure 9. Top image shows a 2D NC stabilized by dense ligand layers capping the top and bottom facets (the bottom capping layer is omitted for clarity). Upon increasing temperature, the 2D ligand monolayers collapse and form tubular micelles that facilitate the growth of 1D NCs, particularly in the presence of dipolar interactions between the NC or MSC building blocks. At even higher temperatures, only 0D NCs or MSCs form. Reproduced from ref 4. Copyright 2017 American Chemical Society.

in the absence of pre-existing templates, provided the ligands exert a strong directive effect by synergistically increasing the stability of the growing MSNS through the formation of densely packed monolayers on specific facets. Moreover, as demonstrated by Robinson and co-workers for CdS MSCs[51] and discussed above in section 2.4, the self-assembly of organic−inorganic mesophases concomitantly with the formation of the MSNSs can kinetically stabilize a specific MSNS by hindering its interaction with the reaction medium, thereby preventing both its growth and redissolution.

The model depicted in Figure 9 is nevertheless unable to explain recent experiments by Talapin and co-workers,[56] which demonstrated that ZnSe MSNSs of progressively higher dimensionality (i.e., 0D, 1D and 2D) are sequentially formed in a heat-up synthesis protocol depending on the final reaction temperature: 120 °C yields 0D MSCs, 130 °C yields 1D MSNWs, and 170 °C yields 2D MSNSs. Very fast heating of the reaction mixture (viz., $Zn(stearate)_2$ and Se in oleylamine and octylamine) to 250 °C (or injection at this temperature) was shown to yield quasi-isotropic ZnSe NCs. The authors of the study verified by SAXS that lamellar mesophases were present at room temperature but melted into an isotropic phase at temperatures above 60 °C, allowing them to exclude templating effects, even though TEM images of samples isolated at early stages showed stacks of triangular NSs identified as ZnSe MSCs entrapped in lamellar mesophases.[56] To rationalize their observations, the authors proposed a unified reaction pathway which, depending on the available

https://doi.org/10.1021/acsmaterialsau.1c00075
ACS Mater. Au 2022, 2, 237−249

thermal energy, could lead to the formation of 0D, 1D, and 2D MSNSs or NCs and bulk crystals (Figure 10).[56] According to this model, at temperatures sufficiently high to allow the energy barrier for isotropic homogeneous nucleation to be overcome, the reaction proceeds through classical nucleation and growth pathways under thermodynamic control, leading to the formation of nearly isotropic NCs. In contrast, under conditions in which the barrier to isotropic nucleation is prohibitively high, the reaction is forced to proceed along pathways with lower nucleation barriers.[56] Therefore, under the heat-up conditions used in their experiments, the reaction started with the formation of MSCs and then sequentially proceeded to 1D MSNWs, thinner 2D wurtzite MSNSs, and finally thicker 2D zinc blende MSNSs as the temperature continued to increase.[56] The dominance of 1D growth at lower temperatures is explained by considering that the formation of 1D wires does not involve any activation barrier, in agreement with arguments based on the classical nucleation theory[56] and with experimental observations.[62]

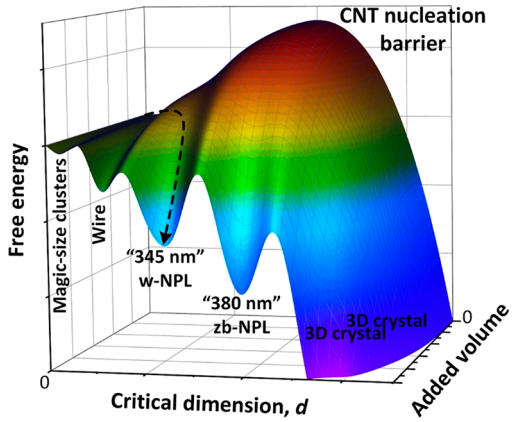

Figure 10. Potential energy landscape for the formation of structures of different dimensionality starting from precursors that form an intermediate magic-sized cluster and then proceed through 1D, 2D, or 3D pathways. An example of the reaction trajectory leading to "345 nm" ZnSe nanoplatelets is shown by the dashed arrow. The numbers between quotation marks indicate the wavelength of the lowest energy exciton absorption peak. The critical dimension represents the smallest dimension for a given shape: diameter for MSCs, nanowires, and spherical NCs, and thickness for nanoplatelets (NPL), which can take either the wurtzite (w) or the zinc blende (zb) structures. The added volume is the total volume of the reaction product added to extend the nanocrystal volume into a 1D nanowire, a 2D nanosheet, or a larger 3D crystal. Reproduced from ref 56. Copyright 2020 American Chemical Society.

It is interesting to note that the models presented in refs 4 and 56 both address the shape evolution of MSNSs but lead to opposite temperature dependences. A possible reason for the discrepancy is that the model depicted in Figure 9 is based on empirical data obtained from reactions carried out by injecting the precursors directly at the reaction temperature,[4] whereas the observations supporting the model depicted in Figure 10 were obtained by heating the precursors to the final reaction temperature.[56] This difference is likely significant, as in the heat-up case, the evolution of the reaction is locked into a trajectory consisting of a chain of sequential events, in which early ones dictate the fate of late ones. For example, 0D MSCs formed at early stages (i.e., lower temperatures) can act as nuclei for both 1D MSNWs and 2D MSNSs. Given that 1D growth has activation energies much lower than those from 2D growth, the former will outcompete the latter for the finite supply of monomers available and will therefore form at lower temperatures. Another important point to consider is that in both cases the monomer formation is likely rate-limiting, as has been demonstrated for several different systems.[63−65] However, in the heat-up strategy employed in ref 56, the impact of the kinetic constraints imposed by the monomer formation will be extended over a longer period and in a temperature-dependent fashion, given that the conversion of precursors to monomers must also overcome an activation barrier. We note that the conditions employed in ref 56 are less favorable for the formation of ligand monolayers due to the dissimilarity in chain lengths between oleylamine and octylamine and the kinked nature of the oleyl chains. This fact should make the van der Waals interactions between the ligand chains less important, in contrast with the assumptions underlying the model presented in Figure 9.

The two models discussed above offer a unified pathway to rationalize the shape and dimensionality of MSNSs but do not explain the quantized growth that typifies them. This latter point has been recently addressed by Norris and co-workers, who also identified correlations between the formation and growth of 2D and 0D MSNSs.[15] Their study showed that a series of tetrahedral zinc blende CdSe magic-sized NCs could be sequentially grown under surface-reaction-limited conditions well beyond the typical MSC size regime (up to 2.7 nm diameter).[15] The authors proposed that the growth from one discrete size to the next occurs in a layer-by-layer fashion, by addition of an entire monolayer to one of the four identical facets of the NCs, so that their tetrahedral shape is preserved.[15] The monomers are initially generated from highly reactive precursors and are quickly consumed by the formation of the first members of the series. Subsequent growth is shown to occur through dissolution of a fraction of the MSNCs, providing monomers for the growth of the remaining MSNCs to the next magic size. A similar process has been previously invoked to explain the ripening of ultrathin CdSe nanoplatelets from one thickness to the next.[15] The additional stability of the magic sizes is explained by the fact that they consist of complete tetrahedra, thereby sitting at local minima in the energy-of-formation curve. Intermediate sizes have incomplete monolayers and are thus unstable.[15]

The sequential, quantized growth through a series of discrete sizes was explained in a similar way for both the 0D and 2D CdSe MSNCs, assuming layer-by-layer growth on nanoscale facets of zinc blende crystallites under surface-reaction-limited conditions.[15] The authors proposed that, under such conditions, the growth rate was dictated by the energy barrier to form a 2D island at a NC facet.[15] For facets smaller than the 2D critical size, the energy barriers (and hence the growth rates, as the formation of the island is the rate-limiting step) become size-dependent, even if all facets are crystallographically identical. Consequently, smaller/thinner facets on NCs are the fastest to grow, outcompeting the others for the limited monomer supply. This results in an ensemble of MSNCs with identical sizes (in the case of tetrahedral 0D NCs) or thicknesses (in the case of 2D NPLs).[15] The transition to the next stable MSNC in the series was thought to occur through dissolution and regrowth. Due to their higher surface to volume ratio, the smaller/thinner MSNCs are also the first to dissolve, providing monomers for the growth of larger/thicker crystallites.[15] The different dimensionalities of

https://doi.org/10.1021/acsmaterialsau.1c00075
ACS Mater. Au 2022, 2, 237−249

0D and 2D MSNCs were assumed to be dictated by the shape of the initial nuclei.[15] Cubic nuclei would evolve into 2D NPLs through stochastic fluctuations at the early stages of the growth, while the self-preserving shape of the tetrahedron would ensure that MSCs evolve into tetrahedral MSNCs if the growth proceeds through a layer-by-layer fashion.

The model proposed in ref 15 thus unifies the formation of 0D MSCs and MSNCs in a single series but postulates a different origin for 2D MSNCs. From this viewpoint, it is inconsistent with the observations reported in ref 56 and with both models discussed above (Figures 9 and 10). The model also does not explain the origin of the differently shaped nuclei that are assumed to evolve into either 0D or 2D MSNCs. It is possible that the differences in the nucleation step are due to the nature of the reaction systems used to yield 0D and 2D zinc blende CdSe MSNCs. In the former case, highly reactive Cd and Se precursors with the elements already in their final oxidation states (viz., bis(stearoyl) selenide and cadmium myristate) are injected in a noncoordinating solvent (1-octadecene) at 240 °C, followed by growth at 180−210 °C.[66] The use of less reactive precursors under otherwise identical conditions was shown to yield regular NCs through continuous growth.[66] In contrast, as discussed in section 4 above, zinc blende CdSe NPLs are obtained under conditions that ensure a high local concentration of precursors. These conditions are experimentally achieved either by adding Se to molten Cd(carboxylates) (regardless of their chain length) or by adding a short-chain Cd(carboxylate) (e.g., cadmium acetate) as a powder to a solution of Se and a long-chain Cd(carboxylate) (e.g., cadmium myristate) in 1-octadecene at 180−240 °C and allowing for growth at 240 °C.[57] It appears to us that the key distinction between the conditions used to obtain 0D or 2D zinc blende CdSe MSNCs is a high (local) concentration of ligands (the Cd-carboxylates) in the latter case. Therefore, as proposed at the end of section 4 above, although the involvement of ligands is not required in the mechanism proposed in ref 15, it seems plausible that they in fact have an adjuvant role, for example, by amplifying kinetic imbalances between otherwise identical facets, by dictating the geometry of the nuclei formed and/or by preventing access to specific facets.

6. CONCLUSION AND OUTLOOK

In summary, despite its long history, research on magic-size colloidal nanostructures is still in its infancy, and many fundamental questions remain unanswered. This relatively slow progress can be attributed to the challenges associated with both the synthesis and isolation of these often-transient species in pure form and their reliable characterization. Moreover, the investigation of different types of magic-size nanostructures (i.e., MSCs, 0D MS nanocrystals, 1D MS nanowires, and 2D MS nanoribbons, nanoplatelets, and nanosheets) has been carried out independently, leading to the development of different fields. Nevertheless, recent years have witnessed great advances in all of these seemingly independent fields, and a unified view is starting to emerge. The observations and considerations discussed in the sections above afford a possible way to integrate the insights offered in the three models discussed in the section 5, allowing us to formulate a plausible answer to the question posed by the title of this Perspective.

From our analysis of the current body of knowledge, it appears that the "magic" originates from the complexity of a dynamic and multivariate system running under reaction-controlled conditions. The "magic" can thus be conjured by emulating appropriate conditions (i.e., suitable combinations of precursors, ligands, concentrations, temperature, etc.), and subsequently kinetically controlled by dynamically manipulating these variables in such a way as to steer the system toward the desired outcome. The best way to visualize the complexity of the potential landscape that emerges from the interplay between these multiple variables under reaction-controlled conditions is to use Figure 10 as a starting point. That figure represents a slice through the dimensionality space under changing temperature and time. A series of coupled local minima will also exist for each of the dimensionalities (0D MSCs and MSNCs, 1D MSNWs, 2D MSNSs) in the direction of increasing critical dimension (be it diameter or thickness) under constant temperature and variable time and also in other directions in the parameter space, such as the ligand or precursor concentration. Under any set of variables, the reaction will be forced to proceed through this continuously changing potential landscape, searching for the pathway with the lowest energy barrier, thereby sequentially forming metastable products as it jumps from one local minimum to the next until it eventually becomes trapped into a minimum that is too deep given the available thermal energy. As a result, depending on the conditions, a 0D MSCs can grow in discrete quantized steps toward larger MSCs, eventually yielding 0D MSQDs, or act as a nonclassical nucleus for 1D MSNWs or 2D MSNPLs, NRBs, and NSs. It may also eventually redissolve and act as a monomer reservoir for continuous growth of regular NCs if the monomer concentration becomes too low and the temperature is sufficiently high.

Nevertheless, the intricacies of this complex interplay between multiple synergistic and antagonistic processes are not yet understood. For example, the exact role of ligands is in most cases obscure. The impact of the precursor to monomer conversion rates and the nature of the species acting as "monomers" also remain elusive. The correlations between the formation mechanisms of 0D, 1D, and 2D MSNSs, their interconversion, and the subtle factors that promote one over the other must yet be fully unravelled. To address these unresolved issues, carefully designed experiments are needed in which several complementary in situ characterization techniques are combined. Fast time-resolved techniques are also required to investigate the early stages of the reaction systems. When satisfactory answers to these knowledge gaps are provided, a truly unified model will be within reach. The "magic" that has been driving the field forward for decades will then finally become "science", allowing the full potential of these nanomaterials to be harvested.

AUTHOR INFORMATION

Corresponding Author

Celso de Mello Donega − *Condensed Matter and Interfaces, Debye Institute for Nanomaterials Science, Utrecht University, 3508 TA Utrecht, The Netherlands;* orcid.org/0000-0002-4403-3627; Email: c.demello-donega@uu.nl

Author

Serena Busatto − *Condensed Matter and Interfaces, Debye Institute for Nanomaterials Science, Utrecht University, 3508 TA Utrecht, The Netherlands*

Complete contact information is available at:

https://doi.org/10.1021/acsmaterialsau.1c00075
ACS Mater. Au 2022, 2, 237−249

https://pubs.acs.org/10.1021/acsmaterialsau.1c00075

Notes

The authors declare no competing financial interest.

■ ACKNOWLEDGMENTS

Financial support from the division of Chemical Sciences (CW) of The Netherlands Organization for Scientific Research (NWO) under Grant No. TOP.715.016.001 is gratefully acknowledged.

■ REFERENCES

(1) Donega, C. de M. Synthesis and Properties of Colloidal Heteronanocrystals. *Chem. Soc. Rev.* **2011**, *40*, 1512−1546.
(2) Reiss, P.; Carrière, M.; Lincheneau, C.; Vaure, L.; Tamang, S. Synthesis of Semiconductor Nanocrystals, Focusing on Nontoxic and Earth-Abundant Materials. *Chem. Rev.* **2016**, *116*, 10731−10819.
(3) Rabouw, F. T.; de Mello Donega, C. Excited-State Dynamics in Colloidal Semiconductor Nanocrystals. *Top. Curr. Chem.* **2016**, *374*, 58.
(4) Berends, A. C.; de Mello Donega, C. Ultrathin One- and Two-Dimensional Colloidal Semiconductor Nanocrystals: Pushing Quantum Confinement to the Limit. *J. Phys. Chem. Lett.* **2017**, *8*, 4077−4090.
(5) Pietryga, J. M.; Park, Y. S.; Lim, J.; Fidler, A. F.; Bae, W. K.; Brovelli, S.; Klimov, V. I. Spectroscopic and Device Aspects of Nanocrystal Quantum Dots. *Chem. Rev.* **2016**, *116*, 10513−10622.
(6) Kagan, C. R.; Lifshitz, E.; Sargent, E. H.; Talapin, D. V. Building Devices from Colloidal Quantum Dots. *Science* **2016**, *353*, aac5523.
(7) Choi, M. K.; Yang, J.; Hyeon, T.; Kim, D. H. Flexible Quantum Dot Light-Emitting Diodes for Next-Generation Displays. *npj Flexible Electron.* **2018**, *2*, 10.
(8) Bourzac, K. Quantum Dots Go on Display. *Nature* **2013**, *493*, 283.
(9) García de Arquer, F. P.; Armin, A.; Meredith, P.; Sargent, E. H. Solution-Processed Semiconductors for Next-Generation Photodetectors. *Nat. Rev. Mater.* **2017**, *2*, 16100.
(10) Xu, J.; Voznyy, O.; Liu, M.; Kirmani, A. R.; Walters, G.; Munir, R.; Abdelsamie, M.; Proppe, A. H.; Sarkar, A.; García de Arquer, F. P.; et al. 2d Matrix Engineering for Homogeneous Quantum Dot Coupling in Photovoltaic Solids. *Nat. Nanotechnol.* **2018**, *13*, 456−462.
(11) Pelaz, B.; Alexiou, C.; Alvarez-Puebla, R. A.; Alves, F.; Andrews, A. M.; Ashraf, S.; Balogh, L. P.; Ballerini, L.; Bestetti, A.; Brendel, C.; et al. Diverse Applications of Nanomedicine. *ACS Nano* **2017**, *11*, 2313−2381.
(12) Won, Y.-H.; Cho, O.; Kim, T.; Chung, D.-Y.; Kim, T.; Chung, H.; Jang, H.; Lee, J.; Kim, D.; Jang, E. Highly Efficient and Stable InP/ZnSe/ZnS Quantum Dot Light-Emitting Diodes. *Nature* **2019**, *575*, 634−638.
(13) Busatto, S.; de Ruiter, M.; Jastrzebski, J. T. B. H.; Albrecht, W.; Pinchetti, V.; Brovelli, S.; Bals, S.; Moret, M.-E.; de Mello Donega, C. Luminescent Colloidal InSb Quantum Dots from In situ-Generated Single-Source Precursor. *ACS Nano* **2020**, *14*, 13146−13160.
(14) Berends, A. C.; Mangnus, M. J. J.; Xia, C.; Rabouw, F. T.; de Mello Donega, C. Optoelectronic Properties of Ternary I-III-VI_2 Semiconductor Nanocrystals: Bright Prospects with Elusive Origins. *J. Phys. Chem. Lett.* **2019**, *10*, 1600−1616.
(15) Pun, A. B.; Mazzotti, S.; Mule, A. S.; Norris, D. J. Understanding Discrete Growth in Semiconductor Nanocrystals: Nanoplatelets and Magic-Sized Clusters. *Acc. Chem. Res.* **2021**, *54*, 1545−1554.
(16) Beecher, A. N.; Yang, X.; Palmer, J. H.; LaGrassa, A. L.; Juhas, P.; Billinge, S. J. L.; Owen, J. S. Atomic Structures and Gram Scale Synthesis of Three Tetrahedral Quantum Dots. *J. Am. Chem. Soc.* **2014**, *136*, 10645−10653.
(17) Hens, Z.; De Roo, J. Atomically Precise Nanocrystals. *J. Am. Chem. Soc.* **2020**, *142*, 15627−15637.
(18) Palencia, C.; Yu, K.; Boldt, K. The Future of Colloidal Semiconductor Magic-Size Clusters. *ACS Nano* **2020**, *14*, 1227−1235.
(19) Friedfeld, M. R.; Stein, J. L.; Cossairt, B. M. Main-Group-Semiconductor Cluster Molecules as Synthetic Intermediates to Nanostructures. *Inorg. Chem.* **2017**, *56*, 8689−8697.
(20) Bootharaju, M. S.; Baek, W.; Lee, S.; Chang, H.; Kim, J.; Hyeon, T. Magic-Sized Stoichiometric II−VI Nanoclusters. *Small* **2021**, *17*, 2002067.
(21) Wang, F.; Wang, Y.; Liu, Y.-H.; Morrison, P. J.; Loomis, R. A.; Buhro, W. E. Two-Dimensional Semiconductor Nanocrystals: Properties, Templated Formation, and Magic-Size Nanocluster Intermediates. *Acc. Chem. Res.* **2015**, *48*, 13−21.
(22) Lee, J.; Yang, J.; Kwon, S. G.; Hyeon, T. Nonclassical nucleation and growth of inorganic nanoparticles. *Nature Rev. Mater.* **2016**, *1*, 16034.
(23) Harrell, S. M.; McBride, J. R.; Rosenthal, S. J. Synthesis of Ultrasmall and Magic-Sized CdSe Nanocrystals. *Chem. Mater.* **2013**, *25*, 1199−1210.
(24) Nasilowski, M.; Mahler, B.; Lhuillier, E.; Ithurria, S.; Dubertret, B. Two-Dimensional Colloidal Nanocrystals. *Chem. Rev.* **2016**, *116*, 10934−10982.
(25) Cossairt, B. M.; Owen, J. S. CdSe Clusters: At the Interface of Small Molecules and Quantum Dots. *Chem. Mater.* **2011**, *23*, 3114−3119.
(26) Groeneveld, E.; van Berkum, S.; van Schooneveld, M. M.; Gloter, A.; Meeldijk, J. D.; van den Heuvel, D. J.; Gerritsen, H. C.; de Mello Donega, C. Highly Luminescent (Zn,Cd)Te-CdSe Colloidal Heteronanowires with Tunable Electron-Hole Overlap. *Nano Lett.* **2012**, *12*, 749−757.
(27) Wang, Y.; Zhou, Y.; Zhang, Y.; Buhro, W. E. Magic-Size II−VI Nanoclusters as Synthons for Flat Colloidal Nanocrystals. *Inorg. Chem.* **2015**, *54*, 1165−1177.
(28) Zhou, Y.; Jiang, R.; Wang, Y.; Rohrs, H. W.; Rath, N. P.; Buhro, W. E. Isolation of Amine Derivatives of $(ZnSe)_{34}$ and $(CdTe)_{34}$. Spectroscopic Comparisons of the $(II−VI)_{13}$ and $(II−VI)_{34}$ Magic-Size Nanoclusters. *Inorg. Chem.* **2019**, *58*, 1815−1825.
(29) Kasuya, A.; Sivamohan, R.; Barnakov, Y.; Dmitruk, I.; Nirasawa, T.; Romanyuk, V.; Kumar, V.; Mamykin, S.; Tohji, K.; Jeyadevan, B.; Shinoda, K.; Kudo, T.; Terasaki, O.; Liu, Z.; Belosludov, R. V.; Sundararajan, V.; Kawazoe, Y. Ultra-Stable Nanoparticles of CdSe Revealed from Mass Spectrometry. *Nat. Mater.* **2004**, *3*, 99−102.
(30) Kudera, S.; Zanella, M.; Giannini, C.; Rizzo, A.; Li, Y.; Gigli, G.; Cingolani, R.; Ciccarella, G.; Spahl, W.; Parak, W. J.; Manna, L. Sequential Growth of Magic-Size CdSe Nanocrystals. *Adv. Mater.* **2007**, *19*, 548−552.
(31) Gaumet, J. J.; Khitrov, G. A.; Strouse, G. F. Mass Spectrometry Analysis of the 1.5 nm Sphalerite-CdS Core of $[Cd_{32}S_{14}(SC_6H_5)_{36}DMF_4]$. *Nano Lett.* **2002**, *2*, 375−379.
(32) Wall, M. A.; Cossairt, B. M.; Liu, J. T. C. Reaction-Driven Nucleation Theory. *J. Phys. Chem. C* **2018**, *122*, 9671−9679.
(33) Dance, I. G.; Choy, A.; Scudder, M. L. Syntheses, Properties, and Molecular and Crystal Structures of $(Me_4N)_4[E_4M_{10}(SPh)_{16}]$ (E = S, Se; M = Zn, Cd): Molecular Supertetrahedral Fragments of the Cubic Metal Chalcogenide Lattice. *J. Am. Chem. Soc.* **1984**, *106*, 6285−6295.
(34) Corrigan, J. F.; Fuhr, O.; Fenske, D. Metal Chalcogenide Clusters on the Border between Molecules and Materials. *Adv. Mater.* **2009**, *21*, 1867−1871.
(35) Soloviev, V. N.; Eichhofer, A.; Fenske, D.; Banin, U. Size-Dependent Optical Spectroscopy of a Homologous Series of CdSe Cluster Molecules. *J. Am. Chem. Soc.* **2001**, *123*, 2354−2364.
(36) Vossmeyer, T.; Reck, G.; Schulz, B.; Katsikas, L.; Weller, H. Double-Layer Superlattice Structure Built Up of $Cd_{32}S_{14}(SCH_2CH(OH)CH_3)_{36}.4H_2O$ Clusters. *J. Am. Chem. Soc.* **1995**, *117*, 12881.

(37) Groeneveld, E.; van Berkum, S.; Meijerink, A.; de Mello Donega, C. Growth and Stability of ZnTe Magic Size Nanocrystals. *Small* **2011**, *7*, 1247−1256.
(38) Gary, D. C.; Flowers, S. E.; Kaminsky, W.; Petrone, A.; Li, X.; Cossairt, B. M. Single-Crystal and Electronic Structure of a 1.3 nm Indium Phosphide Nanocluster. *J. Am. Chem. Soc.* **2016**, *138*, 1510−1513.
(39) Gary, D. C.; Terban, M. W.; Billinge, S. J. L.; Cossairt, B. M. Two-Step Nucleation and Growth of InP Quantum Dots *via* Magic-Sized Cluster Intermediates. *Chem. Mater.* **2015**, *27*, 1432−1441.
(40) Del Ben, M.; Havenith, R. W. A.; Broer, R.; Stener, M. Density Functional Study on the Morphology and Photoabsorption of CdSe Nanoclusters. *J. Phys. Chem. C* **2011**, *115*, 16782−16796.
(41) Martin, T. P. Shells of Atoms. *Phys. Reports* **1996**, *273*, 199.
(42) Williamson, C. B.; Nevers, D. R.; Nelson, A.; Hadar, I.; Banin, U.; Hanrath, T.; Robinson, R. D. Chemically Reversible Isomerization of Inorganic Clusters. *Science* **2019**, *363*, 731−735.
(43) Nevers, D. R.; Williamson, C. B.; Hanrath, T.; Robinson, R. D. Surface Chemistry of Cadmium Sulfide Magic-Sized Clusters: A Window into Ligand-Nanoparticle Interactions. *Chem. Commun.* **2017**, *53*, 2866.
(44) Hsieh, T.; Yang, T.; Hsieh, C.; Huang, S.; Yeh, Y.; Chen, C.; Li, E. Y.; Liu, Y. Unraveling the Structure of Magic-Size $(CdSe)_{13}$ Cluster Pairs. *Chem. Mater.* **2018**, *30*, 5468−5477.
(45) He, L.; Luan, C.; Rowell, N.; Zhang, M.; Chen, X.; Yu, K. Transformations Among Colloidal Semiconductor Magic-Size Clusters. *Acc. Chem. Res.* **2021**, *54*, 776−786.
(46) Palencia, C.; Seher, R.; Krohn, J.; Thiel, F.; Lehmkühler, F.; Weller, H. An *In Situ* and Real Time Study of the Formation of CdSe NCs. *Nanoscale* **2020**, *12*, 22928.
(47) Cossairt, B. M. Shining Light on Indium Phosphide Quantum Dots: Understanding the Interplay Among Precursor Conversion, Nucleation, and Growth. *Chem. Mater.* **2016**, *28*, 7181−7189.
(48) Evans, C. M.; Guo, L.; Peterson, J. J.; Maccagnano-Zacher, S.; Krauss, T. D. Ultrabright PbSe Magic-Sized Clusters. *Nano Lett.* **2008**, *8*, 2896.
(49) Jiang, Z.; Kelley, D. F. Role of Magic-Sized Clusters in the Synthesis of CdSe Nanorods. *ACS Nano* **2010**, *4*, 1561.
(50) Wurmbrand, D.; Fischer, J. W. A.; Rosenberg, R.; Boldt, K. Morphogenesis of Anisotropic Nanoparticles: Self-Templating *via* Non-Classical, Fibrillar Cd_2Se Intermediates. *Chem. Commun.* **2018**, *54*, 7358.
(51) Nevers, D. R.; Williamson, C. B.; Savitzky, B. H.; Hadar, I.; Banin, U.; Kourkoutis, L. F.; Hanrath, T.; Robinson, R. D. Mesophase Formation Stabilizes High-Purity Magic-Sized Clusters. *J. Am. Chem. Soc.* **2018**, *140*, 3652−3662.
(52) Harrell, S. M.; McBride, J. R.; Rosenthal, S. J. Synthesis of Ultrasmall and Magic-Sized CdSe Nanocrystals. *Chem. Mater.* **2013**, *25*, 1199−1210.
(53) Noda, Y.; Maekawa, H.; Kasuya, A. Site Equivalent All Apex 1 nm-Particle of CdSe Preferentially Grown in Solution. *Eur. Phys. J. D* **2010**, *57*, 43−47.
(54) Shen, Q.; Luan, C.; Rowell, N.; Zhang, M.; Wang, K.; Willis, M.; Chen, X.; Yu, K. Reversible Transformations at Room Temperature among Three Types of CdTe Magic-Size Clusters. *Inorg. Chem.* **2021**, *60*, 4243−4251.
(55) Liu, M.; Wang, K.; Wang, L.; Han, S.; Fan, H.; Rowell, N.; Ripmeester, J. A.; Renoud, R.; Bian, F.; Zeng, J.; Yu, K. Probing Intermediates of the Induction Period Prior to Nucleation and Growth of Semiconductor Quantum Dots. *Nature Commun.* **2017**, *8*, 15467.
(56) Cunningham, P. D.; Coropceanu, I.; Mulloy, K.; Cho, W.; Talapin, D. V. Quantized Reaction Pathways for Solution Synthesis of Colloidal ZnSe Nanostructures: A Connection between Clusters, Nanowires, and Two-Dimensional Nanoplatelets. *ACS Nano* **2020**, *14*, 3847−3857.
(57) Riedinger, A.; Ott, F. D.; Mule, A.; Mazzotti, S.; Knüsel, P. N.; Kress, S. J. P.; Prins, F.; Erwin, S. C.; Norris, D. J. An Intrinsic Growth Instability in Isotropic Materials Leads to Quasi-Two-Dimensional Nanoplatelet. *Nat. Mater.* **2017**, *16*, 743.
(58) van der Stam, W.; Rabouw, F. T.; Geuchies, J. J.; Berends, A. C.; Hinterding, S. O. M.; Geitenbeek, R. G.; van der Lit, J.; Prévost, S.; Petukhov, A. V.; de Mello Donega, C. In-Situ Probing of Stack-Templated Growth of Ultrathin $Cu_{2-x}S$ Nanosheets. *Chem. Mater.* **2016**, *28*, 6381−6389.
(59) Salzmann, B. B. V.; van der Sluijs, M. M.; Soligno, G.; Vanmaekelbergh, D. Oriented Attachment: From Natural Crystal Growth to a Materials Engineering Tool. *Acc. Chem. Res.* **2021**, *54*, 787−797.
(60) Schliehe, C.; Juarez, B. H.; Pelletier, M.; Jander, S.; Greshnykh, D.; Nagel, M.; Meyer, A.; Foerster, S.; Kornowski, A.; Klinke, C.; Weller, H. Ultrathin PbS Sheets by Two-Dimensional Oriented Attachment. *Science* **2010**, *329*, 550−553.
(61) Berends, A. C.; Meeldijk, J. D.; van Huis, M. A.; de Mello Donega, C. Formation of Colloidal Copper Indium Sulfide Nanosheets by Two- Dimensional Self-Organization. *Chem. Mater.* **2017**, *29*, 10551−10560.
(62) Chen, J.; Zhu, E.; Liu, J.; Zhang, S.; Lin, Z.; Duan, X.; Heinz, H.; Huang, Y.; De Yoreo, J. J. Building Two-Dimensional Materials One Row at a Time: Avoiding the Nucleation Barrier. *Science* **2018**, *362*, 1135−1139.
(63) Bladt, E.; van Dijk- Moes, R. J. A.; Peters, J.; Montanarella, F.; de Mello Donega, C.; Vanmaekelbergh, D.; Bals, S. Atomic Structure of Wurtzite CdSe (Core)/CdS (Giant Shell) Nanobullets Related to Epitaxy and Growth. *J. Am. Chem. Soc.* **2016**, *138*, 14288−14293.
(64) Hendricks, M. P.; Campos, M. P.; Cleveland, G. T.; Jen-La Plante, I.; Owen, J. S. A Tunable Library of Substituted Thiourea Precursors to Metal Sulfide Nanocrystals. *Science* **2015**, *348*, 1226−1230.
(65) Prins, P. T.; Montanarella, F.; Dümbgen, K.; Justo, Y.; van der Bok, J. C.; Hinterding, S. O. M.; Geuchies, J. J.; Maes, J.; De Nolf, K.; Deelen, S.; Meijer, H.; Zinn, T.; Petukhov, A. V.; Rabouw, F. T.; de Mello Donega, C.; Vanmaekelbergh, D.; Hens, Z. Extended Nucleation and Superfocusing in Colloidal Semiconductor Nanocrystal Synthesis. *Nano Lett.* **2021**, *21*, 2487−2496.
(66) Mule, A. S.; Mazzotti, S.; Rossinelli, A. A.; Aellen, M.; Prins, P. T.; van der Bok, J. C.; Solari, S. F.; Glauser, Y. M.; Kumar, P. V.; Riedinger, A.; Norris, D. J. Unraveling the Growth Mechanism of Magic-Sized Semiconductor Nanocrystals. *J. Am. Chem. Soc.* **2021**, *143*, 2037−2048.

https://doi.org/10.1021/acsmaterialsau.1c00075
ACS Mater. Au 2022, 2, 237−249